

# On the absence of gravitational lensing of the cosmic microwave background

Richard Lieu<sup>1</sup> & Jonathan P.D. Mittaz<sup>1</sup>

*Department of Physics, University of Alabama at Huntsville, Huntsville, AL 35899*

## ABSTRACT

The magnification of distant sources by mass clumps at lower ( $z \leq 1$ ) redshifts is calculated analytically. The clumps are initially assumed to be galaxy group isothermal spheres with properties inferred from an extensive survey. The average effect, which includes strong lensing, is exactly counteracted by the beam divergence in between clumps (more precisely, the average reciprocal magnification cancels the inverse Dyer-Roeder demagnification). This conclusion is independent of the matter density function within each clump, and remains valid for arbitrary values of  $\Omega_m$  and  $\Omega_\Lambda$ . When tested against the cosmic microwave background data, a rather large lensing induced *dispersion* in the angular size of the primary acoustic peaks of the TT power spectrum is inconsistent with WMAP observations. The situation is unchanged by the use of NFW profiles for the density distribution of groups, which led in fact to slightly larger fluctuations. Finally, our formulae are applied to an ensemble of NFW mass clumps or isothermal spheres having the parameters of galaxy *clusters*. The acoustic peak size dispersion remains unobservably large, and is also excluded by WMAP. For galaxy groups, two possible ways of reconciling with the data are proposed, both exploiting maximally the uncertainties in our knowledge of group properties. The same escape routes are not available in the case of clusters, however, because their properties are well understood. Here we have a more robust conclusion: neither the NFW profile nor isothermal sphere profiles are an accurate description of clusters, or important elements of physics responsible for shaping zero curvature space are missing from the standard cosmological model. When all the effects are accrued, it is difficult to understand how WMAP could reveal no evidence whatsoever of lensing by groups and clusters.

## 1. Introduction - observed statistics of galaxy groups

Light as it propagates through the near Universe will encounter inhomogeneities. The motivation which initiated the present paper is to investigate the role played by groups of galaxies in the phenomenon of lensing and global curvature, by using (perhaps for the first time) real observational data. Recently, large databases on groups have become available, including in particular an ESO survey (Ramella et al 2002), from which some general properties of 1,168 groups can be inferred. Specifically concerning the lensing performance of the groups, one needs to know their mass and velocity dispersion. These are shown in Figure 1. We then found the mean virial mass per group to be

$$\overline{M}_{\text{group}} \approx 1.15 \times 10^{14} M_{\odot}. \quad (1)$$

The datum can then be used to estimate the value of  $\Omega_{\text{group}}$ , since these 1,168 systems were identified within a surveyed volume of  $0.0075 \text{ Gpc}^3$  (comoving volume of a pie subtending  $4.69 \text{ sr}$  at the observer and of radius extending to redshift  $z = 0.04$ , in a  $h = 0.71$ ,  $\Omega_m = 0.27$ ,  $\Omega_{\Lambda} = 0.73$  cosmology). Hence the number density of groups is:

$$n_{\text{group}} = n_0 = 1.56 \times 10^{-4} \text{ Mpc}^{-3}, \quad (2)$$

and is in fact a lower limit, because no attempt was made here to correct  $n_{\text{group}}$  for selection effects. Eqs. (1) and (2) point to a mass density of

$$\Omega_{\text{group}} \approx 0.135. \quad (3)$$

Given that most galaxies exist in groups, the value is in agreement with the conclusion of Fukugita (2003) and Fukugita, Hogan, & Peebles (1998), who found (after careful mass budget accountancy) that at low redshifts matter amounting to 50 % the total density of  $\Omega_m \approx 0.27$  is connected with galaxies and galactic environments.

How does such a form of mass concentrations affect the propagation of light? To answer this question, some information about the matter profile in groups is necessary. The limited isothermal sphere model, wherein the internal matter density falls radially as  $1/r^2$  to some cutoff radius  $R$ , is sometimes advocated (Zabludoff & Mulchaey 1998, Mulchaey 2000). In this model the value of  $R$  is related to the total mass  $M$  of the group by the equation

$$\frac{GM}{R} = 2\sigma^2, \quad (4)$$

where  $\sigma$  is the dispersion velocity of the group. Since the median dispersion velocity of the ESO group sample is  $\sigma \approx 270 \text{ km s}^{-1}$  (Ramella et al 2002), Eq. (1) and (3) may be coupled to provide an estimate of the cutoff radius  $\overline{R}$  as  $\overline{R} \approx 3 \text{ Mpc}$ .

## 2. Weak lensing: direct incorporation of galaxy group data

Concerning the observed breakdown of the Universe's total mass density, viz.  $\Omega_\Lambda = 0.73$  dark energy and  $\Omega_m = 0.27$  matter (Bennett et al 2003), while at recent epochs ( $z \sim 1$  or less) the  $\Lambda$  component may remain smooth, the matter is certainly known to be clumped into mass concentrations, with galaxy groups forming an important subclass.

The efforts to date on the global (all sky) influence exerted by weak lensing involve primarily N-body simulations (e.g. Wambsganss et al 1997, Barber 2000), complemented by some development on theoretical methods (Dalal et al 2003). There are, however, two areas of neglect: (a) if groups were adequately represented in previous works, it is doubtful whether direct observational properties were involved; (b) analytical formulae are generally lacking, even though they should be provided to the furthest extent possible - the physics is always much clearer through this approach.

### 3. The mean convergence for nearby and very distant sources

Let the origin of the coordinate system be at the observer, who receives a light signal at world time  $\tau_o$ . Let symbols like  $x$  and  $y$  denote the homogeneous Friedmann-Robertson-Walker (FRW) coordinate distance in the limit when space curvature has the negligible value measured by the microwave background observations (with WMAP being the latest, Bennett et al 2003). Suppose the light was emitted by a source at coordinates  $(x_s, y_s, 0)$  and passed through *en route* at world time  $\tau$  a galaxy group with its center at position  $x$  (i.e.  $c\tau = c\tau_o - x$ ). If the group is an isothermal sphere, its potential function will have the form

$$\Phi(r) = -\frac{GM}{R} \left[ 1 - \ln \left( \frac{r}{R} \right) \right]. \quad (5)$$

Further, assume that the middle ray of a pencil beam skirts by the center of the sphere at physical distance  $b$  ( $< R$ ), equivalent to coordinate distance  $y = b/a(\tau)$ , where  $a(\tau)$  is the Hubble expansion parameter at time  $\tau$ . The light is deflected inwards by an angle

$$\psi = \frac{4GM}{R} \left[ \arccos \left( \frac{b}{R} \right) + \frac{R - \sqrt{R^2 - b^2}}{b} \right], \quad (6)$$

where in Eq. (6) and the rest of this work the speed of light *in vacuo* is set to unity. Note that for  $b \ll R$ ,  $\psi$  reduces to the familiar constant  $\psi = 2\pi GM/R = 4\pi\sigma^2$ .

As a result of the lens, the source appears to us to be at position  $(x_s, y'_s, 0)$ , where

$$y'_s = \frac{yx_s}{x}. \quad (7)$$

The geometry of the situation requires that

$$y_s = y'_s - \psi(x_s - x). \quad (8)$$

The apparent size of the source in the radial direction is affected by an amount in accordance with  $dy'_s - dy_s = (x_s - x)d\psi$ . The apparent size in the azimuthal direction, however, is larger than the true size by the ratio  $y'_s/y_s$ . Hence the effect of the scattering is to increase the *average* angular size  $\theta$  of the source by the fractional amount

$$\eta \equiv \frac{\theta' - \theta}{\theta} \quad (9)$$

which by virtue of Eqs. (7) and (8) may be written as

$$\eta = \frac{(x_s - x)x}{2(1+z)x_s} \left( \frac{\psi}{b} + \frac{d\psi}{db} \right). \quad (10)$$

where in Eq. (10) and the rest of this paper the expansion parameter at epoch  $\tau_0$  is set at  $a_0 = 1$ , and  $z \equiv z(x)$  is the redshift of the lens. This leads to a fractional increase in the energy flux carried by the beam, by the amount  $2\eta$ .

The function  $z(x)$  may be obtained by inverting the equation

$$x = c(\tau_0 - \tau) = \frac{1}{H_0} \int_0^z \frac{dz'}{E(z')}, \quad (11)$$

with

$$E(z) = \frac{H(\tau)}{H_0} = [\Omega_m(1+z)^3 + (1-\Omega_m)]^{1/2}. \quad (12)$$

The result is:

$$z(x) = H_0x + \frac{3}{4}\Omega_m H_0^2 x^2 + \dots, \quad (13)$$

i.e. an expansion of  $z(x)$  as a power series in  $x$ .

In reality the light beam intercepts a random and homogeneous distribution of galaxy groups along the way. To work out the total convergence under the scenario of infrequent multiple scattering, we first write down the probability of the arriving light having encountered a group at position between  $x$  and  $x+dx$ , and impact parameter<sup>1</sup> between  $b$  and  $b+db$ , as  $ndV$ . Here  $n$  and  $dV$  are respectively the number density of groups and a cylindrical volume element, both for the epoch  $\tau$ , i.e.

$$ndV = n(\tau)a(\tau)dx \times 2\pi bdb = 2\pi n_0(1+z)^2 dx bdb. \quad (14)$$

where  $n(\tau) \equiv n(z)$  has the functional form  $n(z) = n_0(1+z)^3$  due to Hubble expansion. In Eq. (14) the properties of the galaxy groups were assumed not to change with redshift. The

---

<sup>1</sup>Strictly speaking  $b$  should be replaced by the distance of closest approach of the original undeflected ray, but in the weak lensing limit where  $\psi x \ll R$  this distinction is unimportant.

validity of this statement is restricted to  $z$  being beneath some maximum redshift. Above the maximum, the evolution of groups must be taken into account. This limiting value of  $z$  seems to be at least  $z \approx 0.5$  from direct observation of groups (Jones et al 2002). From dynamical time considerations, a group cannot evolve significantly within a timescale  $\leq \bar{R}/\sigma \approx 3 \times 10^{17}$  s, corresponding to a redshift exceeding  $z = 1.5$ .

We proceed to calculate the expectation value of  $\eta$ , which is given by

$$\langle \eta \rangle = \sum \eta n \delta V = \int \eta n dV \quad (15)$$

with the integration performed over an entire cylinder wherein lenses are present. By means of Eqs. (6), (10), (14), and (15), we performed the integration over  $b$  to arrive at

$$\langle \eta \rangle = 2\pi^2 GM n_0 \int_0^{x_f} dx [1 + z(x)] \frac{(x_s - x)x}{x_s}, \quad (16)$$

where the assumption is for the furthest lens to have a present epoch distance of  $a_0 x_f = x_f$  (beyond  $x = x_f$  the Universe is too smooth to accomodate galaxy groups as we know them today), and that  $b_{\min} \ll R$ . In obtaining Eq. (16) use was also made of the definite integral

$$\frac{1}{R} \int_0^R \arccos \left( \frac{b}{R} \right) db = 1$$

In Eq. (16) we incorporate the contribution to  $\langle \eta \rangle$  from all types of (galaxy group) mass spheres, each having its own mass  $M$  and number density  $n_0$ , with  $\sum n_0 M = \rho_c \Omega_{\text{groups}}$ , where

$$\rho_c = \frac{3H_o^2}{8\pi G} \quad (17)$$

is the critical density. We can recast the expression for  $\langle \eta \rangle$  as

$$\langle \eta \rangle = \frac{3}{2} \Omega_{\text{groups}} H_0^2 \int_0^{x_f} dx [1 + z(x)] \frac{(x_s - x)x}{x_s}, \quad (18)$$

which is the mean angular magnification of any small patch of sky randomly located at coordinate position  $(x_s, y_s, 0)$ . There are two limiting cases when Eq. (18) simplifies. The first is  $x_s = x_f$ , corresponding to sources embedded within the clumpy environment of the near Universe (e.g. Type 1a supernovae). In this case

$$\langle \eta \rangle = \frac{1}{4} \Omega_{\text{groups}} H_0^2 x_s^2 \left( 1 + \frac{1}{2} H_0 x_s + \frac{9}{20} \Omega_m H_0^2 x_s^2 + \dots \right) \quad (19)$$

The 2nd is  $x_s \gg x_f$ , corresponding to very distant sources which emitted light at a time when the Universe was smooth, the cosmic microwave background (CMB). Here we have

$$\langle \eta \rangle = \frac{3}{4} \Omega_{\text{groups}} H_0^2 x_f^2 \left( 1 + \frac{2}{3} H_0 x_f + \frac{3}{8} \Omega_m H_0^2 x_f^2 + \dots \right). \quad (20)$$

Note the absence of any  $x_s$  dependence in Eq. (20). If corrections due to the finiteness of  $x_f/x_s$  are desired, we remark that the lowest order of such terms equals an additional  $-2x_f/(3x_s)$  within the last pair of parentheses.

#### 4. The exact cancellation between the lensing effect of isothermal spheres and the Dyer-Roeder demagnification

A very interesting result which emerges from the analysis thus far concerns the balance between beam convergence by the clumps and divergence within the subcritical density ‘voids’ between clumps. Take for instance a supernova source, the weak lensing of which is described by Eq. (19). If the ‘voids’ are completely matter-free, i.e.  $\Omega_g = \Omega_m$  in Eq. (19), one would attain maximum  $\langle \eta \rangle$ . Yet, in this same limit, the demagnification  $\epsilon$  of the source caused by propagation through the ‘voids’ will be that of the Dyer-Roeder ‘empty beam’ (Dyer & Roeder 1972), viz.

$$\epsilon = \frac{x'_s - x_s}{x_s}$$

where

$$x_s = \frac{1}{H_0} \int_0^{z_s} \frac{dz}{E(z)} ; \quad x'_s = \frac{1}{H_0} (1 + z_f) \int_0^{z_f} \frac{dz}{(1+z)^2 E(z)}, \quad (21)$$

and  $E(z)$  as defined in Eq. (12). The remarkable fact is that an expansion of  $\epsilon$  in power series of  $x_s$  with the aid of Eq. (13) gives *the same series as Eq. (19) with  $\Omega_g = \Omega_m$* .

This development highlights the advantage of an analytical approach. In an earlier work, Weinberg (1976) considered an  $\Omega_\Lambda = 0$  Universe where all the matter is clumped into point masses, and found that the net magnification is still controlled by the  $\Omega_m$  parameter alone - as if space remained homogeneous. The present conclusion reinforces Weinberg in the more realistic context involving clumps of finite size within a Universe of arbitrary  $\Omega_\Lambda$  and  $\Omega_m$ .

The correspondence between a 100 % clumped Universe and the fully homogeneous Universe, as established above, remains in place even if the clumping is not 100 %. This was shown in a separate paper (Lieu & Mittaz 2004) where we also adopted a more unifying method, using the Sach’s optical equations to handle the two opposing effects under one formalism. A toy model on the physics of this section is given in Appendix A. The formal treatment of average magnification in an inhomogeneous Universe is provided by Kibble & Lieu (2005), where the diversity of averages appropriate to different modes of observations and data analysis methods will be calculated and discussed.

#### 5. The standard deviation - convergence fluctuations

Like the two-point correlation function in galaxy count analysis, the first step towards

an expression for  $\delta\eta$  is to let  $n_i$  be the number of groups with their centers lying within a volume  $\delta V$  labelled positionally by an index  $i$ . Provided  $\delta V$  is sufficiently small that there is no appreciable chance for the centers of two groups to be both inside volume  $i$ , then  $n_i = 0$  or  $n_i = 1$ , i.e.

$$n_i^2 = n_i \quad (22)$$

Moreover, because the distribution of groups in space is a Poisson process, and the location of each group does not affect that of another,  $n_i$  has the following properties concerning its averages:

$$\langle n_i \rangle = n\delta V, \quad \langle n_i^2 \rangle = n\delta V, \quad \langle n_i n_j \rangle = \langle n_i \rangle \langle n_j \rangle = (n\delta V)^2. \quad (23)$$

For each volume there is a corresponding contribution to the convergence. If the  $i^{th}$  cell is occupied, we will have

$$\eta_i = \frac{(x_s - x_i)x_i}{2(1 + z_i)x_s} \left( \frac{\psi_i}{b_i} + \psi'_i \right) \quad (24)$$

as the fractional change in the angular size of the source due to its light passing by this cell ( $\psi' = d\psi/db$ ). The total effect is given by a summation along the light path:

$$\eta = \sum_i n_i \eta_i. \quad (25)$$

Taking the average, we have

$$\langle \eta \rangle = \sum_i \langle n_i \rangle \eta_i = \sum_i n\delta V \eta_i. \quad (26)$$

i.e. one obtains Eq. (15) for  $\langle \eta \rangle$ .

Continuing towards the variance, we need the average value of

$$\eta^2 = \left( \sum_i n_i \eta_i \right)^2 = \sum_i n_i \eta_i^2 + \sum_{i \neq j} n_i n_j \eta_i \eta_j, \quad (27)$$

which is given, after taking into account Eq. (23), by

$$\langle \eta^2 \rangle = \sum_i (n\delta V) \eta_i^2 + \sum_{i \neq j} (n\delta V)^2 \eta_i \eta_j. \quad (28)$$

The variance is now computed in accordance with its definition:

$$(\delta\eta)^2 = \langle \eta^2 \rangle - \langle \eta \rangle^2 = \sum_i [n\delta V - (n\delta V)^2] \eta_i^2. \quad (29)$$

where use was made of Eq. (26) and the fact that the  $\langle \eta \rangle^2$  term cancels unless  $i = j$ . Finally, we note that for small enough  $\delta V$ ,  $(n\delta V)^2 \ll n\delta V$  and may be ignored, so that  $(\delta\eta)^2 = \sum_i n\delta V \eta_i^2$ . If the summation over  $i$  is cast in integral form, we will have

$$(\delta\eta)^2 = \int \eta^2 n dV = 8\pi^3 n_0 \sigma^4 \left[ \ln \left( \frac{R}{b_{\min}} \right) - \frac{8}{\pi^2} \right] \int_0^{x_f} dx \left[ \frac{(x_s - x)x}{x_s} \right]^2, \quad (30)$$

where in going towards the last expression use was made of Eqs. (10) and (14) with the full deflection angle from Eq. (6).

Note that the standard deviation differs from the mean  $\langle \eta \rangle$  in two distinct ways. First, while  $\langle \eta \rangle \propto \Omega_{\text{groups}}$ ,  $(\delta\eta)^2$  is more complicated, being  $\propto n_0 \sigma^4$ . Thus  $(\delta\eta)^2$  is much more governed by the specific properties of the type of isothermal spheres in question. Second, unlike  $\langle \eta \rangle$ , the integration towards  $(\delta\eta)^2$  can be performed exactly for all values of  $x_f$  and  $x_s$ . When this is done, and the variance for groups of various radii and velocity dispersions are summed, the result is

$$(\delta\eta)^2 = \frac{8\pi^3}{3} n_0 x_f^3 \left( 1 - \frac{3x_f}{2x_s} + \frac{3x_f^2}{5x_s^2} \right) \sum_{i,j} \left\{ p_{ij} \sigma_i^4 \left[ \ln \left( \frac{R_j}{b_{\min}} \right) - \frac{8}{\pi^2} \right] \right\}, \quad (31)$$

where  $p_{ij}$  is the probability of finding a group with velocity dispersion  $\sigma_i$  and radius  $R_j$ .

## 6. Application to Type 1a Supernovae - a check against numerical simulations

Utilizing the full statistical properties of the 1,168 galaxy groups observed during the ESO survey (Ramella et al 2002, section 1 and Figure 1), the summation in Eq. (31) was found to have the value

$$\sum_{i,j} \left\{ p_{ij} \sigma_i^4 \left[ \ln \left( \frac{R_j}{b_{\min}} \right) - \frac{8}{\pi^2} \right] \right\} = 2.90 \times 10^{-10} \quad (32)$$

for<sup>2</sup>  $b_{\min} = 10$  kpc and under the convention of unit speed of light. The equation, together with Eqs. (2) and (3), permit an evaluation of the quantities  $\langle \eta \rangle$  and  $\delta\eta$  as given in Eqs. (18) and (30).

We now apply the results to the astrophysical phenomenon of Type 1a supernovae (SN1a), where  $x_f = x_s$  (see the comment after Eq. (18)), both being  $\leq$  a few Gpc, and Eq. (18) reduces to Eq. (19). At redshifts  $z_f = z_s = 1$  and 1.5, the values of  $(\langle \eta \rangle, \delta\eta)$  are

---

<sup>2</sup>At such a small minimum impact parameter the lensing may have become strong, so that readers can legitimately question whether the present calculation, which is based on the assumption of weak lensing, still applies. The answer is yes, and is explained in section 8 and Appendix B

respectively (0.031, 0.036) and (0.060, 0.055). Note in each case  $\delta\eta$  is at most  $\simeq \langle\eta\rangle$  (the same applies also to the CMB - see below). This means in the context of our paper there is no concern over the probability distribution of  $\eta$  becoming asymmetric (skewed). In fact the distribution is truncated only at the tail end of the left wing: because from section 4 it was proved that  $\langle\eta\rangle$  exactly equals the demagnification percentage at the voids, a negative excursion of  $\eta$  from the mean value of  $\langle\eta\rangle$  by one standard deviation  $\langle\eta\rangle - \delta\eta$  does not render the source fainter than the rigid lower bound set by the Dyer-Roeder beam.

In fact, our value of  $2\delta\eta \approx 6\%$  for the brightness fluctuation at  $z = 1$  compares well with that of cosmological N-body simulations by Barber (2000), who obtained 7.8 % (this rather large  $\delta\eta$  may well be the reason why Barber (2000) found an average amplification of -3.4 % when our analytical calculation gives zero). We also quote, for completeness, another result for  $\delta\eta$  from an earlier simulation of Wambsganss et al (1997), whose value was 4 %. The fluctuation is nonetheless still marginal for the purpose of testing against SN1a data, wherein the brightness dispersion is at the 0.35 magnitude level (Barris et al 2004, Tonry et al 2003).

## 7. Application to the CMB - should space be as flat as observed?

Observations of the CMB are much more accurate than those of SN1a, and can be used to conduct a useful test of the standard cosmological model. For the CMB at  $z_s \approx 1000$ , and assuming that the galaxy groups populate the near Universe (without significant evolution) to  $z = z_f$  we have, from Eq. (18),  $\langle\eta\rangle = 0.099$  and 0.157 respectively for  $z_f = 1$  and 1.5. Also, from Eqs. (2), (31), and (32), we find that  $\delta\eta = 0.093$  at  $z_f = 1$  and 0.133 at  $z_f = 1.5$ .

In the present work we focus on  $\delta\eta$ , the dispersion in the angular size of CMB hot and cold spots. Previous attempts in estimating the extent of this effect involved ray tracing codes (e.g. Pfrommer 2003), concerning which it is not entirely clear what galaxy groups properties were assumed, and how well they correspond to observations. The quantity  $\delta\eta$  has the meaning of a standard deviation in the angular size of sources positioned along independent sightlines that sample the variation in the spatial location of different sets of groups. The separation  $\alpha$  between such sightlines is  $\sim$  the angular diameter of a typical group, with present physical radius  $\approx 3$  Mpc (see Eq.(4)), placed midway (in comoving FRW distance scale) between us and  $z = z_f$ , i.e.  $\alpha \approx 12.4$  arcmin for  $z_f = 1$ , and 9.4 arcmin for  $z_f = 1.5$ . Hence if a spherical harmonic in the CMB TT power-spectrum has mean angular size  $\theta = \pi/l$  less than or of order  $\alpha$ , the dispersion in  $\theta$  will simply be

$$\delta\theta = \theta\delta\eta \quad (\theta \leq \alpha, \text{ coherent scattering}). \quad (33)$$

If on the other hand the structure is large, and it contains  $N \sim \theta^2/\alpha^2$  subregions magnified

independently by distinct lens combinations, then intuitively

$$\delta\theta = \frac{\theta\delta\eta}{\sqrt{N}} \quad (\theta > \alpha, \text{ incoherent scattering}), \quad (34)$$

although Eq. (34) may also be established firmly by a mathematical proof, which is provided in Appendix C. In both cases  $\delta\theta$  is to be added in quadrature to the intrinsic dispersion in the structure sizes, which are due to density perturbations at decoupling. The dividing line between the two cases,  $\alpha \approx 10$  arcmin, is to be compared with the value of 20 arcmin advocated by Bartelmann & Schneider 2001 (BS). In fact, if the essential part of our Eq. (31), viz.

$$(\delta\eta)^2 \sim \frac{n_0\sigma^4 L^3}{c^4} \quad (35)$$

where  $L = x_f$ , is converted into the notation of BS, we will make the substitution  $n_0 \rightarrow 1/R^3$  (BS assumed  $L/R$  lenses per distance  $L$ ),  $R \rightarrow 1/k$ ,  $L \rightarrow w$ , and  $\sigma^2/c^2 \rightarrow 2\Phi$ . It will then be clear from Eqs. (33) through (35) that  $\delta\theta$  is  $\approx$  the deflection angle dispersion  $\sigma(\phi)$  of BS for both coherent and incoherent scattering. The key difference, however, is that because for the galaxy groups being considered  $\delta\eta \approx 0.1$ , some five times higher than the corresponding value in BS, one expects significant broadening of the spherical harmonics. As can be seen in Figure 2, such a behavior is inconsistent with the WMAP data.

An immediate check concerns whether the galaxy group properties we derived from the ESO survey are representative of the truth. There are two aspects open to critique. Firstly, the cutoff radius given in Eq. (4) is determined from the virial mass  $M$  and the dispersion velocity  $\sigma$ , the former of which (i.e.  $M$ ) is only an inferred quantity. It is entirely possible that in reality we have a mean cutoff radius  $\bar{R} \ll 3$  Mpc (i.e. the total mass of a typical group is  $\ll$  its virial mass), but the total amount of matter within galaxies and groups constitute an  $\Omega_{\text{group}}$  which still satisfies Eq. (3). This would involve a smaller  $M$  and  $R$  for each group, but a larger number density of groups than the value of Eq. (2). In fact, from an earlier ESO survey Ramella et al (1999) estimated that if observational selection effects were taken into account  $n_{\text{group}}$  could reach  $4 \times 10^{-3}$  Mpc $^{-3}$  (see Figure 6c of Ramella et al 1999, where the number density plotted should be multiplied by  $h^3$ ), i.e. an increase from Eq. (2) by a factor of  $\sim 25$ . To remain in compliance with Eqs. (3) and (4), then, the cutoff radius  $\bar{R}$  (and hence mean angular size  $\alpha$ ) of the groups must both decrease by the same factor, to  $\bar{R} \approx 120$  kpc. Returning to Eqs. (31) and (32), we see that  $\delta\eta$  becomes somewhat higher, but the real difference comes from the  $\sqrt{N}$  reduction factor for incoherent scattering at a given CMB spot size, Eq. (34), which is now 25 times more severe. As a result of these modifications, the net broadening effect on the primary acoustic peaks is kept drastically in check - the theoretical TT power spectrum is no longer distinguishable from that of the standard model (the solid line of Figure 2).

The second way of resolving the observational conflict is to question the legitimacy in our assumption that all the observed groups are virialized systems with the density profile of an isothermal sphere. Strictly speaking, the only relatively secure candidates are those 61 X-ray emitting groups in the ESO survey (Ramella et al 2002), for reasons already explained in section 1. Since these objects constitute  $\approx 5\%$  of the total sample, it could be argued that the actual value of  $\delta\eta$  should involve a reduced number density,  $n_0 \rightarrow 0.05n_0$ , in which case  $\delta\eta$  would become  $\approx 2\%$ , and one recovers the minimal distortion advocated by BS, with a resulting TT power spectrum that differs negligibly from the solid line of Figure 2. With this reduction of  $\delta\eta$ , however, the SN1a brightness dispersion estimate becomes 0.016, closer now to the result of Wambsganss et al (1997) than Barber (2000). One question worthy of consideration is, even if most of the groups are not isothermal spheres, they should still possess some intra-group gravitational potential, so that the present undertaking of ignoring altogether their influence on light may not be justified. Effectively the problem is resolved under this scenario by assuming that groups are nothing more than a collection of individual galaxies which act as a large number of tiny incoherent lenses, thereby minimizing the size dispersion of large light sources.

## 8. Generalization of sections 3 – 5 to clumps of arbitrary internal density profiles

The development of sections 3 – 5 may readily be extended to the case of mass clumps with an arbitrary internal density distribution, with the deflection angle  $\psi(b)$  of Eq. (6) having the general form

$$\psi(b) = 2 \int_{-\infty}^{\infty} \frac{Gm(r)b}{r^3} dx = 4 \int_0^{\pi/2} \frac{Gm(r)}{b} \cos\alpha d\alpha, \quad (36)$$

where  $r = \sqrt{x^2 + b^2} = b \sec\alpha$ , and the mass  $m(r)$  within radius  $r$  can be an arbitrary function of  $r$ . In terms of the density  $\rho(r)$  at  $r$ , where

$$\frac{dm(r)}{dr} = 4\pi r^2 \rho(r), \quad (37)$$

the fractional weak lensing angular magnification reads

$$\eta = \frac{2Gx_l(x_s - x_l)}{(1 + z_l)x_s} \int_b^{\infty} \frac{4\pi r \rho(r) dr}{\sqrt{r^2 - b^2}}. \quad (38)$$

By integrating over the probability element for randomly located clumps,  $dP = ndV$  of Eq. (14), and taking account of the fact that

$$\int_0^{\infty} b db \int_b^{\infty} \frac{4\pi r \rho(r) dr}{\sqrt{r^2 - b^2}} = M, \quad (39)$$

the total mass of each clump, one again arrives at Eq. (18) for the average value of  $\eta$ . Thus the conclusion in section 4 of zero net magnification relative to that in a homogeneous Universe of the same mean density is valid for lensing clumps with any profile  $\rho(r)$ , and is not contingent upon the state of inhomogeneity of the Universe. Moreover, in Appendix B we shall prove that, as long as the meaning of the average is appropriately defined, both this conclusion and Eq. (18) for  $\langle \eta \rangle$  remain unchanged even when the light rays are allowed to pass through clumps at sufficiently small impact parameters where strong lensing effects must also be included.

In fact, the most general treatment of the problem is to be found in Kibble & Lieu (2005), who showed using a more powerful (vierbein) formalism that even under a broader range of circumstances than those enumerated above (a) the Universe may still be regarded as homogeneous concerning the mean properties of its propagating light, *and* (b) Eq. (18) is the correct expression for  $\langle \eta \rangle$ . One advantage of Kibble & Lieu (2005) lies in its utilization of the expansion  $\theta$  of a small ray bundle, which is an additive quantity irrespective of the strength of the lensing.

Since the averaging procedure  $\langle \eta \rangle = \int \eta dP$  is applicable to the full range of  $b$ , large and small, it follows from the derivation of section 5 that the same statement may be made about the convergence fluctuation, viz. it too is always given by the expression  $(\delta\eta)^2 = \int \eta^2 dP = \int \eta^2 n dV$ . Thus, from Eqs. (38) and (14) we deduce that

$$(\delta\eta)^2 = \int \eta^2 n dV = 8\pi n_0 G^2 \int_0^{x_f} dx_l \left[ \frac{(x_s - x_l)x_l}{x_s} \right]^2 \int_0^\infty b db \left[ \int_b^\infty \frac{4\pi r \rho(r) dr}{\sqrt{r^2 - b^2}} \right]^2, \quad (40)$$

for spherical clumps having any  $\rho(r)$ .

## 9. NFW profiles

With the availability of Eq. (40) the way is paved for investigating convergence fluctuation due to the intra-group matter distribution having a profile  $\rho(r)$  which differs from the isothermal sphere. In particular, attention is devoted to the increasingly employed Navarro-Frenk-White or, NFW, model (Dubinski & Carlberg 1991; Navarro et al 1995, 1996, 1997), which involves a function of the form

$$\rho(r) = \frac{\delta_c \rho_c r_s^3}{r(r + r_s)^2} \quad (41)$$

between  $r = 0$  and  $r = R$ , where  $\delta_c$  and  $r_s$  are respectively known as the overdensity factor and scale radius,  $\rho_c$  is as given in Eq. (17), and  $R$  is the virial radius, related to the r.m.s dispersion velocity  $\sigma$  by

$$R = \frac{\sqrt{3}}{10} \frac{\sigma}{H_0 E(z)}, \quad (42)$$

with  $E(z)$  as in equation (12) and  $\sigma$  as a velocity measured in the frame of the cluster, i.e.  $\sigma \sim (1+z)$ . For  $z \leq 1.5$ ,  $(1+z)/E(z)$  is a constant. Hence  $R$  may also be regarded as constant, apart from intrinsic evolution effects which we already argued is without the support of evidence in the case of groups. Moreover, the scale radius  $r_s$  is  $\approx 26\%$  of the virial radius, or

$$\frac{R}{r_s} = 3.846 = c \quad (43)$$

(see Carlberg et al 1997), and the overdensity  $\delta_c$  depends on the ratio  $c$  via the equation

$$\delta_c = \frac{200}{3} \frac{c^3}{\ln(1+c) - \frac{c}{1+c}}. \quad (44)$$

Since we are considering the lensing effects of nearby groups, the modification to  $R$  by the function  $E(z)$  is ignored.

From Eqs. (40) and (41) one arrives at

$$(\delta\eta)^2 = \frac{64\pi^3 n_0 x_f^3}{3} \left[ \left( \frac{GM_0}{b_{\min}} \right)^2 - 2 \left( \frac{GM_0}{R} \right)^2 \ln \left( \frac{R}{b_{\min}} \right) \right] \left( 1 - \frac{3x_f}{2x_s} + \frac{3x_f^2}{5x_s^2} \right), \quad (45)$$

valid for any  $b_{\min}$  except  $b_{\min} \ll r_s$ , where the quantity  $M_0$  is given by

$$M_0 = \delta_c \rho_c r_s^3. \quad (46)$$

For galaxy groups with  $\sigma \approx 270 \text{ km s}^{-1}$  we obtain, from Eqs. (42) to (44), the following NFW model parameters:  $R = 668 \text{ kpc}$ ,  $r_s = 174 \text{ kpc}$ , and  $\delta_c = 4.83 \times 10^4$ . Substituting these values into Eq. (45), we computed  $\delta\eta$  assuming a group density  $n_0$  such that  $n_0 M = \Omega_g$ , where  $M$  is the total mass within the virial radius  $R$ , and  $\Omega_g$  is still given by Eq. (3). This involved assigning  $n_0$  a value  $\approx$  three times higher than that of Eq. (2). Moreover, by setting<sup>3</sup>  $b_{\min} \approx 100 \text{ kpc}$ , we then find that  $\delta\eta$  is about 1.5 times higher than its corresponding value as determined by Eqs. (2), (31) and (32) for isothermal sphere density profiles, when the same distances  $x_f$  and  $x_s$  apply to both cases. Thus one can safely declare that the conclusions of sections 6 and 7 also hold for NFW density profiles.

## 10. The absence of convergence fluctuation in the CMB due to clusters of galaxies

With all the physical and mathematical prerequisites in place, we are ready for the clincher test, which utilizes clusters of galaxies - extensively observed systems with well

---

<sup>3</sup>We conservatively avoid setting  $b_{\min}$  too low, because the performance of NFW profiles in the very inner parts of galaxy groups and clusters is controversial.

determined properties - as gravitational lenses. Nearby clusters have a number density at the present epoch (Bahcall 1988) of

$$n_0 \approx 10^{-5} h^3 \text{ Mpc}^{-3} \quad (47)$$

at  $h = 0.71$ , and a mean velocity dispersion in the cluster frame of (Struble & Rood 1991) of

$$\sigma \approx 1000(1+z) \text{ km s}^{-1}. \quad (48)$$

The latter corresponds, by the low  $z$  version of Eq. (42), to a mean virial radius of

$$R \approx 2.12 \text{ Mpc}, \quad (49)$$

and hence a mean virial mass in the range

$$M = \frac{800\pi}{3} \rho_c R^3 \approx 1.12 \times 10^{15} M_\odot. \quad (50)$$

Moreover, there is ample evidence that clusters do not evolve significantly put to  $z_f \sim 1$  (Hashimoto et al 2002, 2004; Maughan et al 2003; Younger, Bahcall, & Bode 2005), so that once again for our present purposes  $n_0$  and  $R$  may be treated as constants.

Combining equations (40) through (44) with equations (47) and (49), followed by a numerical integration of equation (40) with  $b_{\min} = 100$  kpc,  $x_s \approx 14.02$  Gpc to the CMB, and  $x_f \approx 4.41$  Gpc to the farthest lens (set at  $z_f = 1.5$ ), one obtains  $\delta\eta \approx 10\%$ . Given that nearby clusters have comparable angular sizes as the galaxy groups (both having  $R \approx 2 - 3$  Mpc), i.e. the effect of incoherent lensing is already calculated in section 7, the implication of this result on the TT primary acoustic peaks is again an expected smearing of the gaussians as depicted in Fig. 2 (ignoring a slight skewness in the convolution), which is contradicted by observations.

Alternatively one could return to the isothermal sphere model, with  $\rho(r) = M/(4\pi r^2 R)$  cutting off at  $r = R$ , and the values of  $R$  and  $M$  as given by equations (49) and (50). Then, with the same source-lens distances as in the case of the NFW profile, equation (40) gives also  $\delta\eta \approx 10\%$  at  $b_{\min} = 100$  kpc after a numerical integration, i.e. our conclusion of a conflict between prediction and reality remains.

## 11 Summary and conclusion

The all-sky convergence fluctuation of light by galaxy groups, with properties inferred from an extensive survey of groups, is computed. When applied to Type 1a supernovae brightness - a situation where the effects are generally hard to measure - the results were

found to be in broad agreement with the predictions of earlier authors. When considering the CMB, the consequence of a sizable dispersion in the angular diameter of the temperature fluctuations is more serious, because it does not correspond to the observational reality represented by the latest WMAP data.

There are at least two ways of overcoming the difficulty, both of which point to the possibility that in reality galaxy groups have by far not yet developed to their virial masses and virialized potential. The first one advocates the existence of many more groups than the directly detected ones upon which the analysis in this paper was based. The total number density remains in accordance with the published correction for selection effects (Ramella et al 1999), but the mean mass per group is substantially reduced. The outcome is a great deal more incoherence in the lensing of the primary acoustic peak structures, and any additional dispersion in a spherical harmonic  $\ell$  becomes unobservable. In the second resolution we questioned the actual fraction of the groups within the ESO survey sample which have fully formed isothermal sphere or NFW profiles. If this is estimated by counting only the X-ray emitting groups, the number of such groups is so small that their effect on the CMB will again be beneath the margin of detectability.

Finally, our predicted all-sky variation in the size of the CMB acoustic peaks based upon the lensing effect of clusters of galaxies was compared with WMAP data. This raises the much more serious question on why convergence fluctuations in the size of the second CMB acoustic peak due to clusters are absent. The ‘escape route’ arguments of the previous paragraph, which may have worked in the case of galaxy groups, are no longer so compelling in the present context, simply because rich clusters are very well studied systems. Nevertheless, one could still contemplate a less profound consequence, viz. perhaps the NFW and isothermal sphere profiles are not a good description of clusters after all. Given, however, that the range of impact parameters we used to derive the value of  $\delta\eta$  is optimal for the performance of the profiles, this does not seem to be a sensible way out. We therefore end with the startling conclusion that the large scale curvature of space may not entirely be an initial value problem related to inflation. The absence of gravitational lensing of the CMB point to the possibility that even effects on light caused by wrinkles in the space of the late (nearby) Universe have been compensated for, beyond some distance scale, by a mechanism which maintains a flat geometry over such scales.

Authors are indebted to T.W.B. Kibble for his independent re-deriving and cross-checking of the mathematical formulae in the paper.

## Appendix A - Heuristic model to illustrate the coupling between the influence of clumps and voids on light propagation

We provide a simple way of gaining an insight into why the geometry of space as revealed by light is, to the lowest order of approximation, independent of the state of inhomogeneity of the incipient matter. For the purpose it is only necessary to use non-expanding Euclidean space as starting point, i.e. let space be uniformly flat and empty, so that the propagation of light is governed by null geodesics in a Minkowski background metric. Clumps may be introduced without changing the average properties, by placing at random locations spheres of total mass  $M$  and internal density profiles  $\rho(r)$  extending to a radius  $R$ , with the matter for each sphere being drawn evenly from a concentric cavity of radius  $R_1 \gg R$ . The picture is then rather akin to the ‘swiss cheese’ model. Rays passing at impact parameters  $b > R_1$  behave as if the relevant clump does not exist. At  $R < b \leq R_1$  a ray is deflected inwards by the angle  $\psi_0 = 4GM/b$  because of the clump, and outwards by the angle

$$\psi_1 = -\frac{4GM}{b} \left[ 1 - \frac{(R_1^2 - b^2)^{\frac{3}{2}}}{R_1^3} \right] \quad (A1)$$

because of negative mass distribution in the void. The net inward deflection  $\psi = \psi_0 - \psi_1$  is then given by

$$\psi = \frac{4GM}{R_1^3 b} (R_1^2 - b^2)^{\frac{3}{2}} \text{ for } R < b \leq R_1, \quad (A2)$$

which vanishes at  $b = R_1$ , thereby satisfying the continuity requirement. Lastly, at  $b \leq R$  the clump itself deflects rays inwards according to Eq. (36). With the void included, we have

$$\psi = \frac{4G}{b} \int_0^{\pi/2} m(r) \cos \alpha d\alpha - \frac{4GM}{b} \left[ 1 - \left( 1 - \frac{b^2}{R_1^2} \right)^{\frac{3}{2}} \right], \quad (A3)$$

where  $r = b \sec \alpha$  and  $m(r)$  is the mass within radius  $r$  ( $m(R) = M$ ). Again, the two values of  $\psi$  at the  $b = R$  boundary match.

Next, let the source be at an infinite distance away, and the clump-void system be centered at distance  $x$  from the observer. The angular magnification formula of Eq. (10) reduces, in the present context, to

$$\eta = \frac{x}{2} \left( \frac{\psi}{b} + \frac{d\psi}{db} \right) \quad (A4)$$

Note that when light transits the void region (i.e.  $R < b \leq R_1$ ) there is demagnification - this is the Dyer-Roeder effect. The average weak lensing magnification is obtained by integrating  $\eta$  w.r.t. the probability element appropriate to a random distribution of clump-void systems

of density  $n_0$ , viz.  $dP = 2\pi n_0 bdbdx$ . If the clumpy region spans the range  $x = 0$  and  $x = L$ ,

$$\langle \eta \rangle = 4\pi G n_0 \int_0^L x dx \left[ \int_0^\infty bdb \int_b^\infty \frac{4\pi r \rho(r) dr}{\sqrt{r^2 - b^2}} - \frac{3M}{R_1^2} \int_0^{R_1} \left(1 - \frac{b^2}{R_1^2}\right)^{\frac{1}{2}} bdb \right] = 0, \quad (A5)$$

where Eq. (39) was used to calculate the first term in the square parentheses. Thus, as long as the light signals pass *through* a sufficient number of clumps and voids, the average source size does not deviate from the Euclidean benchmark.

## Appendix B - on how to average the magnification if strong lensing is included

To establish the correct averaging procedure it is only necessary to consider one foreground clump, placed at the center of the field of a large, circular, and uniformly illuminated background source. Take a small annulus of emission, the undeflected and actual light paths connecting it and the observer pass by the clump at impact parameter  $b_0$  and  $b$  respectively. In the weak lensing limit, it is unnecessary to distinguish  $b$  from  $b_0$ . In the absence of the lens, the solid angle subtended by the annulus at the observer is

$$d\tilde{\omega} = (1 + z_l)^2 \frac{2\pi bdb}{x_l^2}.$$

In the presence of the lens  $d\tilde{\omega}$  is increased by the amount  $4\pi(1 + z_l)^2 \eta bdb/x_l^2$  where, according to section 8,  $\eta$  is given by

$$\eta = \frac{L}{2} \left( \frac{\psi}{b} + \frac{d\psi}{db} \right) = 2GL \int_b^\infty \frac{4\pi r \rho(r) dr}{\sqrt{r^2 - b^2}}, \quad (B1)$$

with  $L = x_l(x_s - x_l)/[(1 + z_l)x_s]$ .

If the unlensed source occupies (in projection on the lensing plane) a circular area of physical radius  $B_0$  as measured at  $z = z_l$ , the *average* percentage magnification of its observed solid angle may be expressed as

$$\frac{\delta\tilde{\omega}}{\tilde{\omega}} = \frac{1}{\pi B_0^2} \times 8\pi GL \int_0^\infty bdb \int_b^\infty \frac{4\pi r \rho(r) dr}{\sqrt{r^2 - b^2}} = \frac{8GML}{B_0^2} = 2\langle \eta \rangle, \quad (B2)$$

where in the second last equality used was made of Eq. (39), and in the last equality the average of  $\eta$  is defined as

$$\langle \eta \rangle = \frac{\int_0^B 2\pi \eta bdb}{\int_0^B 2\pi bdb}, \quad (B3)$$

and matches Eqs. (14) and (15) of the main text with  $1/\int 2\pi bdb$  replacing  $n(z)\delta x_l/(1 + z_l)$ , since in this Appendix the number of clumps within a comoving slice at distances  $x_l \rightarrow x_l + \delta x_l$

is exactly one. Note that from Eq. (B2) the percentage magnification depends only on the mass of the enclosed clump - it is not affected by the details of the clump's internal density profile. This is reasonable, because all forms of lensing conserve surface brightness (i.e. no overlap of emission regions in the image possible) the extra solid angle the magnified image claims is simply given by the amount of outward deflection of the 'boundary rays' of the source - a process which relates only to the clump mass - because such rays are too far away from the clump to be mindful of its inner structure.

On the other hand, we know that the above consideration is limited to the regime of weak lensing, so the question is whether inclusion of strong lensing modification of the integrand in Eq. (B1), which is inevitable as one reaches the bottom end of the integration, would lead to new terms carrying extra parameter dependence to jeopardize our hitherto consistent result.

To see why the answer is no, we must now extend the treatment to accomodate the possibility of strong lensing, i.e. the relationship  $b_0 \approx b$  is no longer rigorous enough. Rather, it has to be expressed more precisely as

$$b_0 = b - L\psi(b). \quad (B4)$$

We may define the *reciprocal magnification* of the annulus area by the formula

$$J = \frac{1}{\mu} = \frac{b_0 db_0}{bdb} \quad (B5)$$

We see that while the average *direct* area magnification  $\mu$

$$\langle \mu \rangle = \frac{\int_0^B 2\pi \mu b db}{\int_0^B 2\pi b db}, \quad (B6)$$

with asymptotic boundary parameters related by

$$B_0 = B - L\psi(B) = B - \frac{4GML}{B}, \quad (B7)$$

is divergent because at sufficient low  $b$  one encounters the caustic  $J = 0$  which is clearly not a weak lensing phenomenon, the average of  $J = 1/\mu$  is free from infinity problems. Thus our undertaking to evaluate the average reciprocal magnification is not motivated by the need to obtain the 'desired' outcome, but to obtain a meaningful outcome. Explicitly

$$\langle J \rangle = \left\langle \frac{1}{\mu} \right\rangle = \frac{\int_0^B 2\pi J b db}{\int_0^B 2\pi b db} = \frac{B_0^2}{B^2}, \quad (B8)$$

where in reaching the last expression use was made of the fact that  $J$  is the Jacobian of transformation from  $bdb$  to  $b_0db_0$ . Note also from Eqs. (B3), (B6), and (B8) that the calculation of all the averages are consistent.

The average percentage magnification of the image area, including the effect of strong lensing of the central rays, is now equal to  $\langle J \rangle^{-1} - 1 = (B^2 - B_0^2)/B_0^2$ . By Eq. (B7), this is just  $8GML/B_0^2$ , in agreement with Eq. (B2). We succeeded in proving that the formula for  $\langle \eta \rangle$  in Eq. (B3), which as explained in the material immediately following this equation reflects exactly the same averaging procedure adopted in the main text of the entire paper, is appropriate to the full regime of weak and strong lensing. Therefore, *the statistical cancellation between lensing magnification and the Dyer-Roeder beam, sections 4 and 8, is a robust conclusion not contingent upon the strength of the lensing*. Our Eq. (40) for the variance  $(\delta\eta)^2$  is, for this reason, also valid at arbitrarily low impact parameters.

Those interested in ‘seeing beyond the mathematics’ to actually understand how the numerator integral for  $\langle J \rangle$  in Eq. (B8) yields  $\pi B_0^2$  despite the presence of multiple images in strong lensing should consider in detail how the integration is carried out in  $b_0$  space. Specifically, in Eq. (B4)  $b_0$  does not change monotonically with  $b$ . As the latter decreases there comes a place, say  $b = b_1$ , at which the corresponding  $b_0 = b_{10} = 0$ . After this, initially for  $b < b_1$ ,  $b_0$  turns negative. For any non-singular central density function  $\rho(r)$ , however,  $\psi(b) \rightarrow 0$  as  $b \rightarrow 0$ , so when  $b$  decreases further from  $b = b_1$  towards  $b = 0$  a point  $b = b_2$  will come at which  $b_0$  reaches a minimum of  $b_0 = b_{20}$ , thereafter increasing again towards  $b_0 = 0$ . Obviously  $J = 0$  at both  $b = b_1$  and  $b = b_2$ . Within the strong lensing regime, then, there are in general three images of any given source pixel, as is well known. The first one corresponds to  $b > b_1$ , and is on the same side of the center (on-axis position) as the source pixel. The second and third images correspond to  $b_2 < b < b_1$  and  $0 < b < b_2$  respectively, and lie on the opposite side. For the first and third image,  $J > 0$ ; for the second,  $J < 0$ . The  $J$ -integral may therefore be separated into three, viz.

$$\int_0^B 2\pi J b db = \int_{b_1}^B 2\pi J b db + \int_{b_2}^{b_1} 2\pi J b db + \int_0^{b_2} 2\pi J b db. \quad (B9)$$

Changing variable to  $y = |b_0|$  and applying Eq. (B5), one may see how the integration takes place in  $b_0$  space, with the sign of  $J$  for the three images assuming particular importance:

$$\int_0^B 2\pi J b db = \int_0^{B_0} 2\pi y dy - \int_0^{|b_{20}|} 2\pi y dy + \int_0^{|b_{20}|} 2\pi y dy = \pi B_0^2, \quad (B10)$$

in agreement with Eq. (B8).

## Appendix C: On the convergence fluctuation of a large source

Like the problem in Appendix B, the necessary theorem here may be established by considering only one slice of redshift. Within this slice let us introduce transverse coordinates  $\vec{y}$  and suppose that for one clump at  $\vec{y}_1$  the value of  $\eta$  for a small bundle of light rays at  $\vec{y}$  is given by  $\eta(\vec{y}) = f(\vec{y} - \vec{y}_1)$ . If the number of clumps per unit area is  $n$ , the average of  $\eta$  will be

$$\bar{\eta}(\vec{y}) = n \int f(\vec{y} - \vec{y}_1) d^2 \vec{y}_1. \quad (C1)$$

If the averaging is performed over a sufficiently large area  $\bar{\eta}(\vec{y}) = \langle \eta \rangle$  should become independent of  $\vec{y}$ . Moreover, the equation

$$(\delta\eta)^2 = n \int f^2(\vec{y}) d^2 \vec{y}. \quad (C2)$$

gives, by section 5, the variance in  $\langle \eta \rangle$ .

It's also useful to define the correlation function  $\xi(\vec{y})$  via

$$(\delta\eta)^2 \xi(\vec{y}) = n \int f(\vec{y}') f(\vec{y} + \vec{y}') d^2 \vec{y}'. \quad (C3)$$

Clearly,  $\xi(\vec{0}) = 1$ , and  $\xi(\vec{y})$  falls off with  $y$  on a scale characteristic of the size of a clump. We can therefore write

$$A_1 = \int \xi(\vec{y}) d^2 \vec{y}. \quad (C4)$$

as *definition* of the area  $A_1$  of a clump.

To calculate the mean and variance in the magnification of a background source of projected area  $A$  at the lensing plane, let us first consider the effect of all the clumps in a really large area  $S \gg A$ . The probability that within  $S$  there are exactly  $\mathcal{N}$  clumps at the positions  $\vec{y}_1, \dots, \vec{y}_{\mathcal{N}}$ , say, within small areas  $d^2 \vec{y}_1, \dots, d^2 \vec{y}_{\mathcal{N}}$ , is given by the Poisson distribution

$$d^{2\mathcal{N}} P = e^{-nS} n^{\mathcal{N}} \prod_{j=1}^{\mathcal{N}} d^2 \vec{y}_j. \quad (C5)$$

The total increase in the area of  $A$  due to lensing by these clumps is  $2\eta_A A$  where

$$\eta_A A = \int_A d^2 \vec{y} \sum_{j=1}^{\mathcal{N}} f(\vec{y} - \vec{y}_j). \quad (C6)$$

To find the average, we integrate (C6) over the measure (C5), and sum over  $\mathcal{N}$ . The result is

$$\langle \eta_A \rangle A = \int_A d^2 \vec{y} e^{-nS} \sum_{\mathcal{N}=1}^{\infty} \frac{n^{\mathcal{N}}}{\mathcal{N}!} \int_S d^2 \vec{y}_1 \dots d^2 \vec{y}_{\mathcal{N}} \sum_{j=1}^{\mathcal{N}} f(\vec{y} - \vec{y}_j). \quad (C7)$$

Note that the  $\mathcal{N}!$  factor is needed to compensate for multiple counting of permutations of the clumps. Also, as already explained in Appendix B, this averaging procedure has correctly taken into account strong lensing effects as well. Thus we obtain

$$\bar{\eta}_A = e^{-nS} \sum_{\mathcal{N}=1}^{\infty} \frac{n^{\mathcal{N}-1}}{(\mathcal{N}-1)!} S^{\mathcal{N}-1} \langle \eta \rangle \left[ \frac{1}{A} \int_A d^2 \vec{y} \right] = \langle \eta \rangle, \quad (C8)$$

where in reaching Eq. (C8) we observe that each  $\int_S d^2 \vec{x}_i$  term in the summation over  $j$  in Eq. (C7) gives the same contribution: one of the integrals over  $\vec{x}_i$  yields, by Eq. (C1),  $\langle \eta \rangle / n$ , and the others altogether yield  $S^{\mathcal{N}-1}$ .

Concerning the average of  $\eta_A^2$ , we now have to take the square of Eq. (C7) and integrate over the measure of Eq. (C6), i.e.

$$\langle \eta_A^2 \rangle A^2 = \int_A d^2 \vec{y} \int_A d^2 \vec{y}' e^{-nS} \sum_{\mathcal{N}=1}^{\infty} \frac{n^{\mathcal{N}}}{\mathcal{N}!} \int_S d^2 \vec{y}_1 \dots d^2 \vec{y}_{\mathcal{N}} \sum_{j,k=1}^{\mathcal{N}} f(\vec{y} - \vec{y}_j) f(\vec{y}' - \vec{y}_k). \quad (C9)$$

In Eq. (C9) it is necessary to separate the terms with  $j = k$  from the others. All terms with  $j \neq k$  are equal, totalling

$$e^{-nS} \sum_{\mathcal{N}=2}^{\infty} \frac{n^{\mathcal{N}-2}}{(\mathcal{N}-2)!} S^{\mathcal{N}-2} \langle \eta \rangle^2 \int_A d^2 \vec{y} \int_A d^2 \vec{y}' = \langle \eta \rangle^2 A^2, \quad (C10)$$

i.e. these terms add up to the very quantity that needs to be subtracted from  $\langle \eta_A^2 \rangle A^2$  to obtain the variance. The variance is then simply given by the sum total of all the  $j = k$  terms. We arrive at

$$(\delta \eta_A)^2 A^2 = e^{-nS} \sum_{\mathcal{N}=1}^{\infty} \frac{n^{\mathcal{N}-1}}{(\mathcal{N}-1)!} S^{\mathcal{N}-1} \int_A d^2 \vec{y} \int_A d^2 \vec{y}' \int_S d^2 \vec{y}_1 n f(\vec{y} - \vec{y}_1) f(\vec{y}' - \vec{y}_1). \quad (C11)$$

By Eq. (C3) we have, finally,

$$(\delta \eta_A)^2 A^2 = (\delta \eta)^2 \int_A d^2 \vec{y} \int_A d^2 \vec{y}' \xi(\vec{y}' - \vec{y}). \quad (C12)$$

Defining  $N = A/A_1$  as the ratio of the source area to the clump area, then, so long as  $N$  is large (i.e. away from the  $N \leq 1$  regime)  $\vec{y}$  will not be too near the boundary, and the integral over  $\vec{y}'$  will give  $A_1$ , while the remaining integral over  $\vec{y}$  is  $= A$ . Thus, apart from small (boundary-effect) corrections,

$$(\delta \eta_A)^2 = (\delta \eta)^2 \frac{A_1}{A} = \frac{(\delta \eta)^2}{N}. \quad (C13)$$

## References

Bahcall, N. 1988, ARAA, 26, 631.

Barber, A.J., 2000, MNRAS, 318, 195.

Barris, B.J. et al 2004, ApJ, 602, 571.

Bartelmann, M. & Schneider, P., 2001, Physics Reports, 340, 291.

Bennett, C.L. et al, 2003, ApJS, 148, 1-27.

Carlberg, R.G. et al 1997, ApJ, 485, L13.

Dalal, N., Holz, D.E., Chen, X., & Frieman, J.A., 2003, ApJ, 585, L11.

Dubinski, J., & Carlberg, R.G. 1991, ApJ, 378, 496.

Dyer, C.C., & Roeder R.C., 1972, ApJ, 174, L115.

Fukugita, M., 2003, in ‘Dark matter in galaxies’, IAU Symp. 220, Sydney (astro-ph/0312517).

Fukugita, M., Hogan, C.J., & Peebles, P.J.E., 1998, ApJ, 503, 518.

Hashimoto, Y., Barcons, X., Boehringer, H., Fabian, A.C.,  
Hasinger, G., Mainieri, V., Brunner, H., 2004, A & A, 417, 819.

Hashimoto, Y., Hasinger, G., Arnaud, M., Rosati, P., Miyaji, T., 2002, A & A, 381, 841.

Jones, L.R., McHardy, I., Newsom, A., Mason, K, 2002, MNRAS, 334, 219.

Kibble, T.W.B., & Lieu, R., 2005, ApJ, submitted (astro-ph/0412275).

Lieu, R., & Mittaz, J.P.D., 2004, ApJL submitted (astro-ph/0409048).

Maughan, B.J., Jones, L.R., Ebeling, H., Perlman, E., Rosati, P.,  
Frye, C., Mullis, C.R., 2003. ApJ, 587, 589.

Mulchaey, J, 2000, ARAA, 38, 289.

Navarro, J.F., Frenk, C.S., & white, S.D.M. 1995, MNRAS, 275, 56.

Navarro, J.F., Frenk, C.S., & white, S.D.M. 1996, ApJ, 462, 563.

Navarro, J.F., Frenk, C.S., & white, S.D.M. 1997, ApJ, 490, 493.

Pfrommer, C., 2002, Cosmological weak lensing of the cosmic microwave background  
by large scale structures, Diploma Thesis, Friedrich-Schiller Universität Jena.

Ramella, M., Geller, M.J., Pisani, A., & da Costa, L.N., 2002, AJ, 123, 2976.

Ramella, M. et al, 1999, A & A, 342, 1.

Tonry, J.L. et al 2003, ApJ, 594, 1.

Wambsganss J., Cen, R., Xu, G, & Ostriker, J.P., 1997, ApJ, 475, L81.

Weinberg, S., 1976, ApJ, 208, L1.

Younger, J.D., Bahcall, N.A., Bode, P., 2005, ApJ, 622, 1.

Zabludoff, A.I., & Mulchaey, J.S., 1998, ApJ, 496, 39.

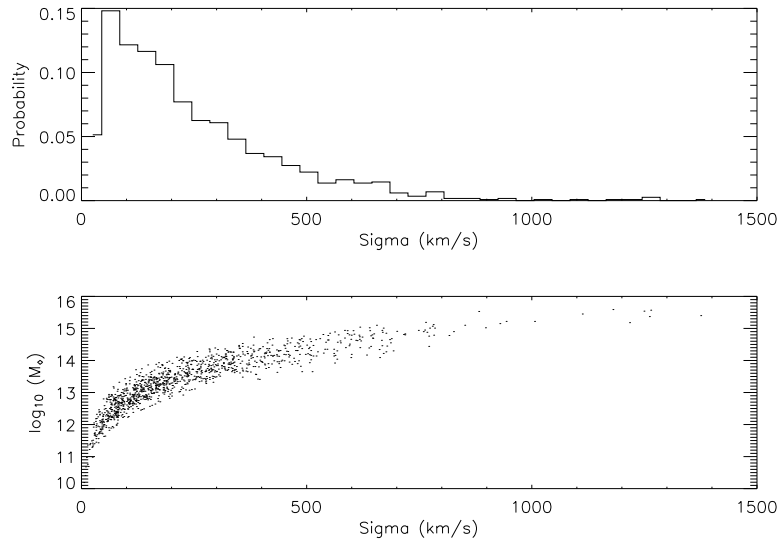


Fig. 1.— The probability distribution of galaxy group velocity dispersion (top panel) and the distribution of group mass against velocity dispersion (bottom panel), both derived from the ESO survey (Ramella et al 2002). These data have been used to evaluate the quantity  $\sum_{i,j} p_{ij} \sigma_i^4 \ln(R_j/b_{min})$  of Eq. (31).

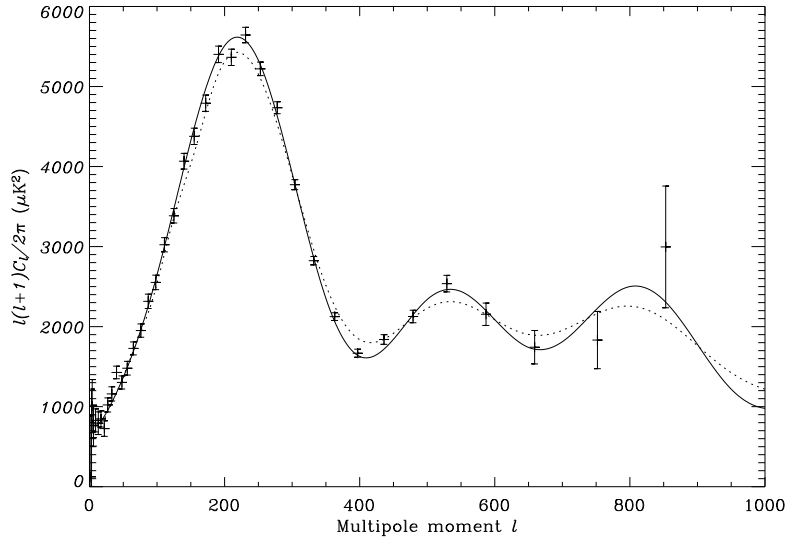


Fig. 2.— The standard FRW model with  $h = 0.71$ ,  $\Omega_m = 0.27$ ,  $\Omega_\Lambda = 0.73$  as applied to the TT power spectrum measured by WMAP is plotted as a solid line. If in this model 50 % of the matter within  $z \approx 1$  is clumped into isothermal spheres with properties given by the ESO survey of galaxy groups, the lensing induced convergence fluctuation ( $\delta\eta \approx 10\%$ ) will cause a smearing of the spherical harmonics at and around the primary acoustic peaks by an amount in accordance with Eqs. (33) and (34). The resulting theoretical power spectrum is plotted as a dashed line - it is an unacceptable fit to the data, with  $\chi^2_{\text{red}} = 2.42$  for 38 degrees of freedom (null probability hypothesis  $< 0.0001$ ).